

WE provide evidence for anisotropic diffusion in rat corpus callosum and hippocampus. The preferential diffusion pathway in corpus callosum is along the myelinated axon fibres; in the hippocampus diffusion is easier along the transversal axis (x) than along the sagittal (y) or vertical (z) axes. In all areas studied, i.e. in the cortex, corpus callosum and hippocampus, the mean ECS volume fraction α ($\alpha = \text{ECS volume}/\text{total tissue volume}$) ranged between 0.20 and 0.22 and mean non-specific uptake k' was between 4.0 and $5.9 \times 10^{-3} \text{ s}^{-1}$. Diffusional anisotropy in the hippocampus may be of importance for extrasynaptic transmission and in the 'cross-talk' between synapses. *NeuroReport* 9: 1299–1304 © 1998 Rapid Science Ltd.

Key words: Anisotropy; Apparent diffusion coefficient; Extracellular space; Extrasynaptic transmission; Tortuosity; Volume fraction

Diffusion heterogeneity and anisotropy in rat hippocampus

Tomáš Mazel, Zuzana Šimonová and Eva Syková^{CA}

Department of Neuroscience, 2nd Medical Faculty, Charles University, V úvalu 84, Prague 150 18; Department of Neuroscience, Institute of Experimental Medicine AS CR, Vídeňská 1083, Prague 142 20 Czech Republic

^{CA}Corresponding Author

Introduction

Extrasynaptic transmission, mediated by the diffusion of neuroactive substances (including ions, neurotransmitters, neuromodulators, growth factors and other macromolecules) through the extracellular space (ECS), plays an important role in short- and long-distance communication between neurons, axons and glia.^{1–3} Recently, hypotheses concerning glutamate 'spillover' and cross-talk between synapses, in which diffusion might play an important role, have been formulated, and experimental evidence for their existence was found in the hippocampus.^{4–6} The hippocampus is well-known for its role in memory formation.⁷ Not only its importance but also its well-defined structure render it suitable for computational modelling where extracellular space size and geometry might be important parameters.

So far the majority of studies in the hippocampus have used methods that only allow for the estimation of relative changes in the ECS volume.³ Some studies used radioactive tracers to measure the ECS volume fraction.⁸ Two studies used the real-time iontophoretic TMA⁺ (tetramethylammonium) method, which allows one to calculate absolute values of the ECS volume as well as the apparent diffusion coefficient (ADC). These studies, performed in brain slices, detected a heterogeneity between CA1, CA3 and dentate gyrus, and unusually low values of the ECS volume fraction α ($\alpha = \text{ECS volume}/\text{total tissue volume}$) were reported in the CA1 region (0.119 in the stratum pyramidale, 0.132 in the stratum

radiatum).^{9,10} However, the authors did not take into account potential anisotropy, i.e. the possibility that diffusion in one direction might be easier than in other directions. If diffusion in a particular brain region is anisotropic, then the correct value of extracellular space volume fraction cannot be calculated from measurements made in only one direction. For anisotropic diffusion the diagonal components of the tortuosity tensor are not equal and generally its non-diagonal components need not be zero. Nevertheless, if a suitable frame of reference is chosen (i.e. if we measure in three privileged orthogonal directions), neglecting the non-diagonal components becomes possible and the correct size of the ECS can thus be determined.¹¹ Anisotropy has been already demonstrated in corpus callosum,¹² spinal cord white matter¹³ and in cerebellum.¹¹ Anisotropic diffusion would allow for some degree of specificity in extrasynaptic transmission. Diffusion in the brain also attracts ever-increasing interest as diffusion-weighted MRI helps in the early diagnosis of cerebral infarct and other pathological states of the CNS.¹⁴

Our study is the first *in vivo* measurement of extracellular space diffusion parameters in the hippocampus. We addressed the question whether anisotropic diffusion of substances occurs in the mammalian hippocampus and whether the unusually low values of the ECS volume⁹ are correct. Therefore, we measured TMA⁺ diffusion in the ECS independently in three orthogonal axes (x , transverse; y , sagittal; z , vertical).

Materials and Methods

Experiments were performed on 18 male 3- to 5-month-old Wistar rats (weight 310–500 g). Rats were anaesthetized with sodium pentobarbital (65 mg/kg, i.p.) and additional small doses were used to maintain anaesthesia during the experiment. The skull was opened with a dental drill 3–4 mm caudal from the bregma, 2–3 mm lateral from the midline, and the dura removed. The animal was secured in a stereotaxic apparatus on a heated platform to maintain body temperature at 37–38°C. Artificial cerebrospinal fluid¹⁶ containing 1 mM TMA chloride heated to 37°C was continually dripped onto the surface of the exposed skull to make a small pool over the brain surface. The animals breathed spontaneously.

The real-time iontophoretic TMA⁺ method¹⁵ was used to determine extracellular space volume fraction $\alpha = \text{ECS volume}/\text{total tissue volume}$, tortuosity $\lambda = (D/\text{ADC})^{0.5}$, where D is the free diffusion coefficient and ADC is the apparent diffusion coefficient of TMA⁺ in the brain, and non-specific uptake k' . The tortuosity factor describes how the migration of molecules is slowed down by pore geometry, macromolecules or fixed negative surface charges. TMA⁺ is a small cation (mol. wt 74.1) that is restricted to the extracellular compartment and mimics the extracellular diffusion of small neuroactive molecules, ions and metabolites. The real-time iontophoretic method is based on fitting the time-dependent rise and fall of the extracellular concentration of TMA⁺ to a radial diffusion equation modified to account for extracellular volume fraction and tortuosity.¹⁵

Double-barrelled ion-selective electrodes were fabricated as described previously.^{12,16,17} The tip of the ion-sensing barrel was filled with K⁺ exchanger (Corning 477317), and the rest of the channel was back-filled with 100 mM TMA chloride. The reference barrel contained 150 mM NaCl. Iontophoretic micropipettes were prepared from theta tubes. After pulling, the micropipette was bent so that it could be aligned parallel to that of the ion-selective microelectrode and was back-filled with 100 mM TMA chloride. An electrode array was made by gluing together a TMA⁺-selective microelectrode and two iontophoresis micropipettes with a tip separation of 100–200 μm in such a way that the tips of the micropipettes and the TMA⁺-selective microelectrode formed a right angle, allowing us to measure simultaneously in either x and y (Fig. 1), x and z , or y and z directions. Typical iontophoresis parameters were +20 nA bias current (continuously applied to maintain a constant transport number), with +80 nA current steps of 60 s duration to generate the diffusion curve (Fig. 1).

Potentials recorded with the reference barrel were subtracted from the TMA⁺-selective barrel voltage measurements by means of buffer and subtraction amplifiers. TMA⁺ diffusion curves were captured on a digital oscilloscope (Nicolet 310) and then transferred to a PC-compatible, 486 computer, where they were analysed by fitting the data to a solution of the diffusion equation using the program VOLTORO (Nicholson C., unpublished).

TMA⁺ concentration *vs* time curves were first recorded in 0.3% dilute agar gel (Difco, Agar Noble) in 150 mM NaCl, 3 mM KCl and 1 mM TMA chloride to determine the transport number (n) and the free TMA⁺ diffusion coefficient (D). For the *in vivo* measurements the reference baseline (voltage corresponding to 1 mM TMA⁺) was first read in solution above the brain and then the array was lowered 500 μm beneath the brain surface where the first diffusion curves were recorded. Further recordings were made at 200 μm steps until a depth of 3500 μm was reached. The diffusion curves obtained from various layers of the cortex and hippocampus were analysed to yield the volume fraction α , tortuosity $\lambda_x, \lambda_y, \lambda_z$ in three perpendicular directions and the non-specific uptake term, k' (s^{-1}). These three parameters were extracted by a non-linear curve fitting simplex algorithm operating on the diffusion curve described by equation (1), which represents the behavior of TMA⁺ when the iontophoresis current is applied for duration S . In this expression, C_i is the extracellular concentration of the ion at time t and distance r_i from the source in direction i (j and k being perpendicular to i). The equation governing the diffusion in brain tissue is:¹¹

$$C_i = G_i(t) \quad t < S \text{ for the rising phase of the curve}$$

$$C_i = G_i(t) - G_i(t - S) \quad t > S \text{ for the falling phase of the curve.}$$

The function $G_i(u)$ is evaluated by substituting t or $t - S$ for u in the following equation:

$$\begin{aligned} G_i(u) = & (Q\lambda_j\lambda_k/8\pi D\alpha r_i) \\ & \times \{\exp[r_i\lambda_i(k'/D)^{1/2}] \\ & \times \text{erfc}[r_i\lambda_i/2(Du)^{1/2} + (k'u)^{1/2}] \\ & + \exp[-r_i\lambda_i(k'/D)^{1/2}] \\ & \times \text{erfc}[r_i\lambda_i/2(Du)^{1/2} - (k'u)^{1/2}]\} \end{aligned} \quad (1)$$

The quantity of TMA⁺ delivered to the tissue per second is $Q = In/zF$, where I is the step increase in current applied to the iontophoresis electrode, n is the transport number, z is the number of charges associated with substance iontophoresed (+1 here) and F is Faraday's electrochemical equivalent. The function 'erfc' is the complementary error function.

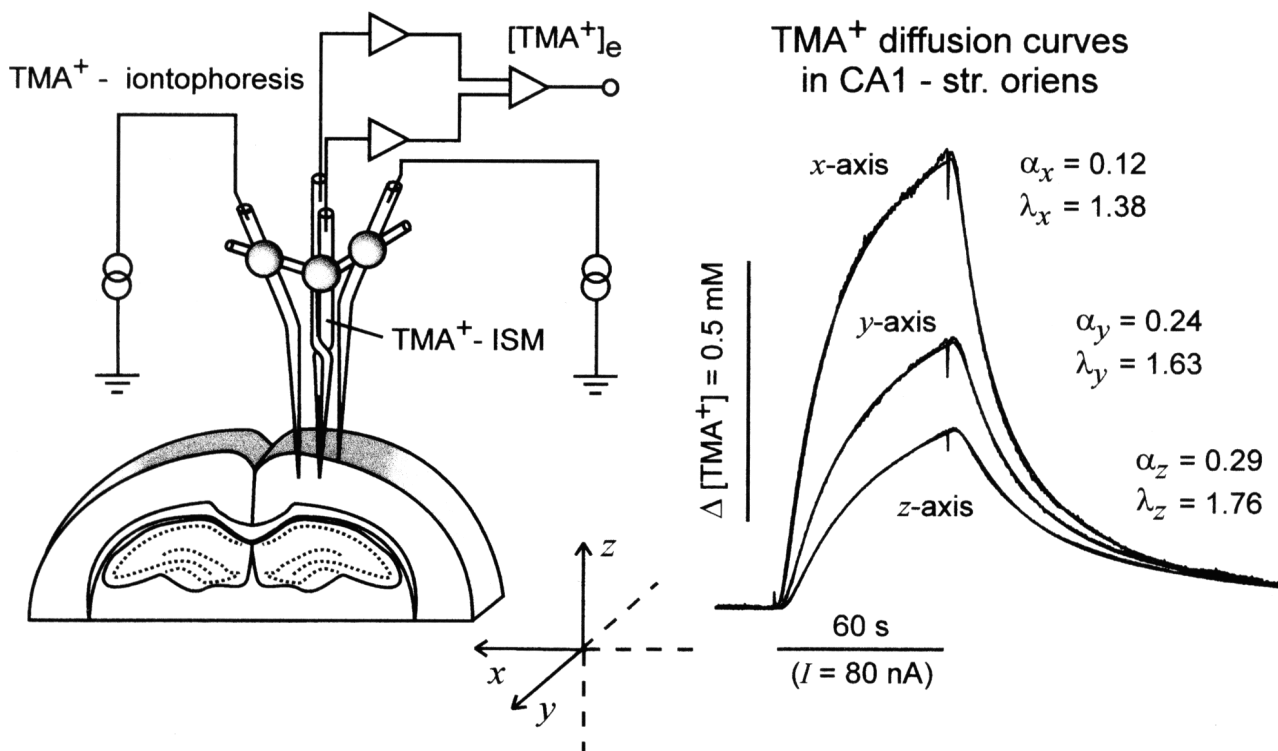


FIG. 1. Experimental setup and typical diffusion curves in the hippocampus. Left: Schema of the experimental arrangement. A TMA⁺-selective double-barreled microelectrode was glued to two iontophoresis microelectrodes to allow for simultaneous measurements in the *x*- and *y*-axes. Right: Anisotropic diffusion in CA1-stratum oriens. TMA⁺ diffusion curves (concentration–time profiles) were measured along three orthogonal axes (*x*, transverse; *y*, sagittal; *z*, vertical). The array spacing *r* was 150, 156 and 158 μm, and transport number (*n*) 0.270, 0.287 and 0.272 in the *x*, *y* and *z* directions, respectively. The slower rise and fall in the *y* than in the *x* direction and even slower in the *z* direction mean higher tortuosity and more restricted diffusion. The amplitude of the curves shows that TMA⁺ concentration, at approximately the same distance from the tip of the iontophoresis electrode, is much higher along the *x* direction than along the *y* and *z* axes. This can be explained if we realize that TMA⁺ concentration decreases with the 'diffusion distance' from the iontophoretic micropipette and that the real 'diffusion distance' is not *r* but λr . Thus the actual or 'diffusion' array spacing is 207, 257 and 275 μm in the *x*, *y* and *z* directions, respectively. The α_x , α_y and α_z values determine the volume fraction that would correspond to the size of the particular diffusion curve if the diffusion were isotropic, i.e. in the case of α_x if the curves in the *y* and *z* directions were of the same height and shape. Note, that the actual ECS volume fraction α is about 0.2 and can be calculated using eqn. 2.

When the experimental medium is agar, by definition, $\alpha = 1 = \lambda$ and $k' = 0$, and the parameters *n* and *D* are extracted by the curve fitting. Knowing *n* and *D*, the parameters α , λ and k' can be obtained when the experiment is repeated in the brain.

The volume fraction α has to be calculated using all three curves. In our measurements we obtained the following values: α_x , α_y , α_z , λ_x , λ_y , λ_z . α was then calculated using the following expressions:

$$\alpha = \alpha_x (\lambda_y \lambda_z / \lambda_x^2) = \alpha_y (\lambda_x \lambda_z / \lambda_y^2) = \alpha_z (\lambda_x \lambda_y / \lambda_z^2) \quad (2)$$

After the experiment the microelectrode array was again calibrated in agar gel to make sure that its characteristics had not changed during the experiment. Animals were perfused, their brains were examined histologically and the position of the microelectrode track was determined.

Results

Three ECS diffusion parameters α , λ and k' were measured in the cortex, corpus callosum (CC) and

hippocampus in three perpendicular axes: *x* (transverse), *y* (sagittal) and *z* (vertical) (Fig. 1). In agreement with our previous developmental study,¹² diffusion in adult rat cortex was isotropic (Table 1), while in corpus callosum it was anisotropic with preferential diffusion along the *x*-axis ($\lambda_x = 1.47$). Diffusion was slowed down along the *y*- and *z*-axes ($\lambda_y = 1.67$, $\lambda_z = 1.69$).

Diffusion anisotropy was found in the hippocampus. It was more pronounced in CA1 than in CA3 and dentate gyrus (DG). The results are summarized in Table 1, showing that whereas tortuosity differs between individual areas, volume fraction tends to be approximately constant (0.20–0.22). Diffusion is preferential along the *x*-axis and significantly slower along the *y*-axis and *z*-axis. In CA1 and CA3 diffusion along the *z*-axis is significantly slower still than along the *y*-axis. The uptake term also differs being lower in CA1 than in CA3.

Figure 1 shows diffusion curves obtained in the CA1-stratum oriens along three perpendicular axes. These three diffusion curves have different ampli-

Table 1. ECS diffusion parameters in adult rat cortex, corpus callosum and hippocampus.

Depth (μm)	Structure	<i>n</i>	α	λ_x	λ_y	λ_z	k' (10^{-3} s^{-1})
500	Cortex layer III	20	0.22 ± 0.01	1.62 ± 0.01	1.64 ± 0.04	1.56 ± 0.04	4.1 ± 0.4
700	Cortex layer IV	17	0.22 ± 0.01	1.61 ± 0.02	1.65 ± 0.01	1.60 ± 0.03	5.9 ± 0.4
900	Cortex layer V	24	0.21 ± 0.01	1.60 ± 0.01	1.59 ± 0.03	1.59 ± 0.03	4.7 ± 0.6
1100	Cortex layer V	34	0.22 ± 0.01	1.57 ± 0.02	1.62 ± 0.02	1.61 ± 0.03	5.4 ± 0.3
1300	Cortex layer V	54	0.22 ± 0.01	1.61 ± 0.01	1.62 ± 0.01	1.57 ± 0.02	5.1 ± 0.3
1500	Cortex layer VI	47	0.21 ± 0.01	1.58 ± 0.02	1.61 ± 0.02	1.62 ± 0.02	5.0 ± 0.3
1700	Corpus callosum	39	0.21 ± 0.01	1.46 ± 0.02	$1.67 \pm 0.03^*$	$1.66 \pm 0.02^*$	4.6 ± 0.3
1900	Corpus callosum	31	0.21 ± 0.01	1.49 ± 0.02	$1.68 \pm 0.03^*$	$1.72 \pm 0.02^*$	4.2 ± 0.3
2100	CA1 stratum oriens + pyramidale	50	0.21 ± 0.01	1.39 ± 0.02	$1.65 \pm 0.04^*$	$1.80 \pm 0.03\#$	4.0 ± 0.3
2300	CA1 stratum radiatum	54	0.22 ± 0.01	1.52 ± 0.02	$1.61 \pm 0.03^*$	$1.82 \pm 0.04\#$	4.4 ± 0.3
2500	CA1 stratum radiatum	48	0.22 ± 0.01	1.50 ± 0.02	1.56 ± 0.02	$1.80 \pm 0.05\#$	4.2 ± 0.3
2700	CA1 stratum lacunosum moleculare	48	0.22 ± 0.01	1.50 ± 0.02	$1.60 \pm 0.03^*$	$1.70 \pm 0.05^*$	4.8 ± 0.3
2900	GD inner blade	47	0.22 ± 0.01	1.49 ± 0.02	$1.59 \pm 0.03^*$	$1.68 \pm 0.05^*$	4.7 ± 0.4
3100	CA3	50	0.22 ± 0.01	1.50 ± 0.03	$1.62 \pm 0.02^*$	$1.69 \pm 0.04^*$	5.2 ± 0.3
3300	CA3	42	0.20 ± 0.01	1.53 ± 0.03	1.58 ± 0.03	$1.70 \pm 0.04\#$	5.5 ± 0.4
3500	GD outer blade	20	0.20 ± 0.01	1.51 ± 0.06	1.64 ± 0.04	$1.73 \pm 0.06^*$	5.3 ± 0.6

Data are expressed as mean \pm s.e.m. *Significantly higher than λ_x ($p < 0.05$); #significantly higher than λ_x and λ_y .

tudes corresponding to the three different values of α_x (0.11), α_y (0.24) and α_z (0.29). However, the real volume fraction α has to be calculated using all three diffusion curves (see expression 2). The curve obtained in the x direction is the highest, with a value of α_x (0.119) as reported previously,⁹ and also has the fastest rise and fall; this means that the diffusion path in this direction is shorter (i.e. tortuosity is lower) though the actual distance between the electrode tips is the same in all cases. Diffusion in the x direction is thus facilitated whereas diffusion in the y direction is restricted and in the z direction is more restricted still. In anisotropic tissue the values of α_x , α_y and α_z are substantially different from the actual ECS volume fraction α . It is therefore evident that neglecting anisotropy and measuring α in only one direction must lead to incorrect values.

Figure 2 shows two histological sections with identified tracks of the microelectrode array. The measurements were always made in two axes simultaneously. Figure 2A shows a coronal section in an animal where measurements were made in the x - and z - axes; Fig. 2B, is a sagittal section in an animal where the measurements were made in the y - and z - axes. The two-dimensional pattern of diffusion away from a point source can be illustrated by constructing iso-concentration circles (isotropic diffusion) and ellipses (anisotropic diffusion) for extracellular TMA⁺ concentration. The circles and ellipses shown in Fig. 2 represent the locations where TMA⁺ concentration reached 0.1, 0.2, 0.3, 0.4, 0.5, 0.6, 0.7, 0.8, 0.9 and 1 mM (represented in grey scale) 60 s after the initiation of a 80 nA iontophoresis current. We used the actual values obtained in two experiments where the electrodes were aligned in the x and z direction (Fig. 2A) and the y and z direction (Fig. 2B). The

smaller the ECS volume fraction, the larger the circle or ellipse. It is evident that circles and ellipses in cortex, corpus callosum and hippocampus are approximately of the same size, suggesting that the ECS volume fraction is not significantly different. However, circles in the cortex reflect the ability of particles to diffuse equally along the x -, y - and z - axes; the ellipses in white matter and in the hippocampus reflect different abilities of substances to diffuse along the x -, y - and z -axes.

Discussion

This is the first study of anisotropic extracellular diffusion in adult rat cortex, corpus callosum and hippocampus using the TMA⁺ method. We confirm previous findings in developing rat brain that diffusion is isotropic in the cortex and anisotropic in the corpus callosum with preferential diffusion along the myelinated fibers.¹² Our results are, however, in disagreement with previous studies in hippocampal slices. These studies reported a very low volume fraction α , mainly in the CA1 region.^{9,10} These values largely correspond to the value of α_x that we obtained in the x direction, whereas if we take into account measurements in the other two directions we obtain a value of α similar to the values in the cortex and corpus callosum. The explanation of the low values of α in previous studies might therefore be that the authors did not consider the possible anisotropy of the hippocampus and that the measurements were not done in all three axes. Moreover, measurements done *in vitro* could be burdened with possible artifacts resulting from the propensity of some areas of the hippocampus to anoxia. However, there might be some disadvantages with our *in vivo* technique,

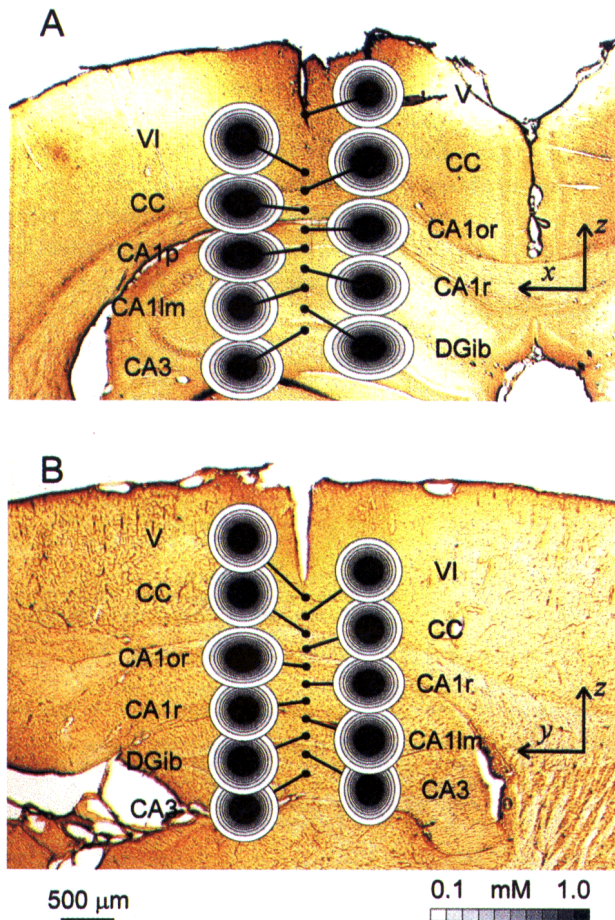


FIG. 2. Two-dimensional isoconcentration plots of extracellular TMA⁺ concentration 60 s after iontophoretic application of TMA⁺, superimposed on GFAP-stained histological sections with identified microelectrode tracks. A coronal (A) and a sagittal (B) section from two animals where measurements were made simultaneously in the x- and z-axis (A) and in the y- and z-axis (B) were immunohistochemically stained for the astrocyte marker GFAP (glial fibrillary acidic protein) and the microelectrode track was identified. The isoconcentration plots were calculated using the actual diffusion parameters (α , λ and k) obtained at various depths of these two identified tracks. Gray densities represent different concentrations of TMA⁺ from 0.1 to 1.0 mM reached 60 s after the onset of iontophoretic application (80 nA) of TMA⁺ in the middle of the circle or ellipse ($D = 1.311 \times 10^{-9} \text{ m}^2 \text{ s}^{-1}$ at 37°C, $n = 0.300$). Ellipses show that diffusion anisotropy was found in corpus callosum and hippocampus. V, VI, cortical layers; CC, corpus callosum; CA1_{or}, CA1-stratum oriens; CA1_p, CA1-stratum pyramidale; CA1_r, CA1-stratum radiatum; CA1_{lm}, CA1-stratum lacunosum moleculare; DG_{ib}, dentate gyrus-inner blade.

including the influence of anesthesia, the imprecise localization of the electrode array, and the possible influence of the barriers that separate corpus callosum from CA1 and CA1 from DG. However, there exist persuasive arguments against such concerns. A number of studies in the cortex have been performed both *in vivo*^{16,18,19} and *in vitro*¹⁰ and no significant differences were found.² This fact favors the hypothesis that *in vivo* measurements are not, to any appreciable degree, influenced by anesthesia. Concerning the problem of the localization of the electrode track, all animals were perfused and exam-

ined histologically and the electrode tracks were found (e.g. see Fig. 2). The main problem might be the correlation of a particular depth with a particular structure. In all our experiments measurements were made in 200 μm steps starting at a depth of 500 μm . We recognize that there might be some 50–150 μm imprecision in recognizing the brain surface. However, the first anisotropic values were always in the corpus callosum. Another important control point in all the tracks was an extremely low value of both λ_x and α_x at a depth of 2100 or 2300 μm . From the comparison of our histological preparations with a stereotaxic atlas²⁰ we chose to locate this point to the dorsal layers of the CA1 area of the hippocampus (alveus, stratum oriens and stratum pyramidale), again the imprecision being about 100 μm . Therefore, though the depth profile is quite accurate, the assignment of a particular structure to an individual depth might be shifted by about 100 μm . Addressing the problem of the influence of barriers separating individual structures, mainly in the hippocampus, we should emphasize that all diffusion parameters must be regarded as averages over the area separating the tips of the iontophoretic micropipette and TMA⁺-sensitive microelectrode, i.e. over a distance of 100–200 μm . In some cases the measurement in the z direction when penetrating from corpus callosum to CA1 gave a very high tortuosity. We suppose that in this case the iontophoresis micropipette was in the corpus callosum and the measuring electrode in CA1. These measurements were excluded from the statistics but are important in suggesting that there is an almost impermeable diffusion barrier separating these two structures.

One of the most surprising results of the present study is the almost constant ECS volume fraction in all the studied structures. Similar values have been found in most CNS areas, including spinal cord¹³ and striatum,³ and even in different species such as mice (Mazel, unpublished results), frogs (Prokopová, unpublished results) and turtles.¹¹ ECS volume fraction changes, however, occur in many pathological situations: an increase in the case of inflammation, demyelination^{2,21} or in transplants,²² and a decrease in the case of anoxia and ischemia.¹⁸ Volume fraction is also different in early postnatal development^{16,18} and in aged animals.²³

Tortuosity is influenced by many factors which we presently cannot separate. These might include membrane barriers including neuronal and glial cell processes, myelin sheaths, macromolecules including the extracellular matrix, molecules with fixed negative surface charges, extracellular space size and pore geometry. Our recent studies support a role for the macromolecular content of the extracellular fluid²⁴ and for geometrical constraints (an increase in

tortuosity accompanied astrogliosis evoked by radiation injury,²¹ astrogliosis²² in grafted tissue and myelination).^{12,13}

Structural anisotropy in some regions of the brain has also been inferred from diffusion-weighted MRI (DW-MRI) measurements.²⁵ DW-MRI, which measures the ADC of water, cannot, however, distinguish between the intra- and extracellular compartments, and therefore these studies could not confirm the extent of anisotropy in the extracellular space.³ In the hippocampus diffusion in the *z* direction is significantly slower than in the *x* and *y* directions. We suppose that there are two main factors contributing to this anisotropy. First, most fiber systems in the hippocampus (Schaffer collaterals in CA1 and mossy fibers in CA3) run transversally. This would, similarly to the corpus callosum,¹² cause higher tortuosity in both the *y*- and *z*-axes. λ_y and λ_z are, indeed, significantly higher than λ_x in all areas of the hippocampus. A second factor that might explain the difference between λ_z and λ_y is that the typical arrangement of cellular aggregates in the hippocampus is in sheets in the *x*-*y* plane, perpendicular to the *z*-axis. These sheets might form diffusion barriers.

It may be of interest that the average tortuosity (averaging λ_x , λ_y and λ_z) is again approximately the same in all areas studied (ranging from 1.60 to 1.65). This means that if a molecule spent a certain time moving in the *x* direction, then the same time in the *y* and *z* directions, it would travel approximately the same distance in all the areas studied. This supports the view that the differences in tortuosity are mainly due to major geometrical constraints (the shape of cells and their processes) rather than the macromolecular content of the extracellular fluid or fixed negative surface charges.

Conclusion

Diffusion in the ECS is the underlying mechanism of extrasynaptic or 'volume' transmission and inter-

cellular, particularly neuron-glia, communication.¹⁻³ Anisotropy may help to facilitate the diffusion of neurotransmitters and neuromodulators to regions occupied by their high affinity receptors, located extrasynaptically. The anisotropy of the ECS in the hippocampus and corpus callosum may, therefore, allow for some specificity of extrasynaptic transmission. It might also be of importance for 'cross-talk' between synapses and for LTP and LTD.⁴⁻⁶

References

1. Agnati LF, Zoli M, Stromberg I and Fuxe K. *Neuroscience* **69**, 711-726 (1995).
2. Syková E. *Neuroscientist* **3**, 28-41 (1997).
3. Nicholson C and Syková E. *Trends Neurosci* (in press).
4. Kullmann DM, Erdemli G and Asztely F. *Neuron* **17**, 461-474 (1996).
5. Asztely F, Erdemli G and Kullmann DM. *Neuron* **18**, 281-293 (1997).
6. Kullmann DM and Asztely F. *Trends Neurosci* **21**, 8-14 (1998).
7. Rolls ET. *Hippocampus* **6**, 601-620 (1996).
8. Rees S, Cragg BG and Everitt AV. *J Neurol Sci* **53**, 347-357 (1982).
9. McBain CJ, Traynelis SF and Dingledine R. *Science* **249**, 674-677 (1990).
10. Pérez-Pinzon MA, Tao L and Nicholson C. *J Neurophysiol* **74**, 565-573 (1995).
11. Rice ME, Okada YC and Nicholson C. *J Neurophysiol* **70**, 2035-2044 (1993).
12. Voříšek I and Syková E. *J Neurophysiol* **78**, 912-919 (1997).
13. Prokopová Š, Vargová L and Syková E. *NeuroReport* **8**, 3527-3532 (1997).
14. Le Bihan D, Turner R and Patronas N. Diffusion MR imaging in normal brain and in brain tumors. In: Le Bihan D, ed. *Diffusion and Perfusion Magnetic Resonance Imaging*. New York: Raven Press, 1995: 134-140.
15. Nicholson C and Phillips JM. *J Physiol (Lond)* **321**, 225-257 (1981).
16. Lehmenkühler A, Syková E, Svoboda J et al. *Neuroscience* **55**, 339-351 (1993).
17. Syková E, Svoboda J, Šimonová Z et al. *Neuroscience* **70**, 597-612 (1996).
18. Voříšek I and Syková E. *J Cerebr Blood Flow Metab* **17**, 191-203 (1997).
19. Cserr HF, De Pasquale M, Nicholson C et al. *J Physiol (Lond)* **442**, 277-295 (1991).
20. Paxinos G and Watson C. *The Rat Brain in Stereotaxic Coordinates*. San Diego: Academic Press, 1997.
21. Šimonová Z, Svoboda J, Orkand P et al. *Physiol Res* **45**, 11-22 (1996).
22. Roitbak T, Mazel T, Šimonová Z et al. *Eur J Neurosci (Suppl)* **9**, 37 (1996).
23. Syková E, Mazel T and Roitbak T. *Soc Neurosci Abstr* **22**, 1495 (1996).
24. Prokopová Š, Nicholson C and Syková E. *Physiol Res* **45**, 28 (1996).
25. Moseley ME, Cohen Y, Kucharczyk J et al. *Radiology* **176**, 439-445 (1990).

ACKNOWLEDGEMENTS: Supported by grants GACR 309/96/0884, GACR 307/96/K226 and IGA MZ 3423-3, GACR 309/97/K048.

**Received 19 January 1998;
accepted 17 February 1998**